

PROCEEDINGS OF SPIE

SPIDigitalLibrary.org/conference-proceedings-of-spie

Solid-state characterization of CdTe: Sn as a medium for adaptive interferometry

Konstantin Shcherbin, Serguey Odoulov, Dean R. Evans,
François Ramaz, Bernard Briat

Konstantin Shcherbin, Serguey Odoulov, Dean R. Evans, François Ramaz, Bernard Briat, "Solid-state characterization of CdTe:Sn as a medium for adaptive interferometry," Proc. SPIE 10934, Optical, Opto-Atomic, and Entanglement-Enhanced Precision Metrology, 109341H (1 March 2019); doi: 10.1117/12.2514823

SPIE.

Event: SPIE OPTO, 2019, San Francisco, California, United States

Solid-state characterization of CdTe:Sn as a medium for adaptive interferometry

Konstantin Shcherbin*^a, Serguey Odoulov^a, Dean R. Evans^b, François Ramaz^c, and Bernard Briat^c

^aInstitute of Physics, National Academy of Sciences, Prospekt Nauki 46, 03680 Kiev, Ukraine

^bAir Force Research Laboratory, Materials and Manufacturing Directorate, Wright-Patterson Air Force Base, OH 45433, USA; ^cInstitut Langevin, Ondes et Images, ESPCI Paris, PSL Research University, CNRS UMR 7587, INSERM U979, Université Paris VI-Pierre et Marie Curie, 1 rue Jussieu, 75005 Paris, France

ABSTRACT

Two-wave mixing adaptive interferometer based on photorefractive crystal allows for compensation of temporal disturbances in ambient environment and operation with speckled beams. The crystal should exhibit large effective trap density, low dark conductivity and large photoconductivity. Deliberately doped semiconductor may meet these requirements. In the present work the photorefractive, spectroscopic and magneto-optical study of CdTe:Sn is performed aiming to estimate these characteristics and to describe the space-charge formation. The photon energies for optical ionization/neutralization of the tin ions are estimated. The crystal is characterized as a medium for two-wave mixing adaptive interferometer with excellent performance.

Keywords: Cadmium telluride, photorefractive effect, photorefractive semiconductor, two-wave mixing, adaptive interferometer, doped semiconductor

1. INTRODUCTION

Adaptive interferometers based on two-wave mixing (TWM) on dynamic holograms allows for remote detection of surface vibrations caused by ultrasonic waves. They can process speckled beams scattered from rough surfaces and compensate for ambient environmental perturbations. Furthermore they can be made to operate intrinsically in quadrature without need for external path length stabilization. In such interferometers a dynamic grating serves as an adaptive beam-splitter¹⁻³. As the grating is dynamic, it adapts to the relatively slowly varying wave front of the object beam caused by undesired external perturbations, ensuring continuous compensation for them. However, the grating may be considered as being fixed for the fast phase variations related to ultrasonic vibrations, thereby enabling conversion of phase modulation to intensity modulation.

The adaptive interferometers have been demonstrated with dynamic gratings recorded in different materials and devices including liquid crystal light valves⁴ and gain medium⁵. The operation with digital holography has also been studied⁶. If digital holography is still clearly inferior to its analog form⁷, dynamic holograms in photorefractive crystals appear to be the most relevant to the application⁸. Among all photorefractive materials, only fast photorefractive semiconductors can compensate for the full bandwidth of mechanical and optical disturbances in the outside ambient because of their short response time⁹. An additional significant advantage of photorefractive semiconductors is their sensitivity in the near infrared. This makes them compatible with many available lasers and telecommunication components.

Photorefractive recording involves a chain of different physical processes^{10,11}. When a photorefractive crystal is illuminated by an interference pattern formed by the recording beams, more free charge carriers are photoexcited from donors in the bright fringes, as it is shown schematically in Fig. 1. The carriers diffuse in the dark areas where they are trapped by charge acceptor states. As a result a spatial charge distribution $\rho(x)$ is created. Owing to the Pockels effect, the electric field of the space-charge $E_{SC}(x)$ induces a refractive index modulation $\Delta n(x)$. In this way the index grating is created. The recording light diffracts from the grating giving rise to different optical effects and various applications¹⁰⁻¹².

*kshcherb@iop.kiev.ua

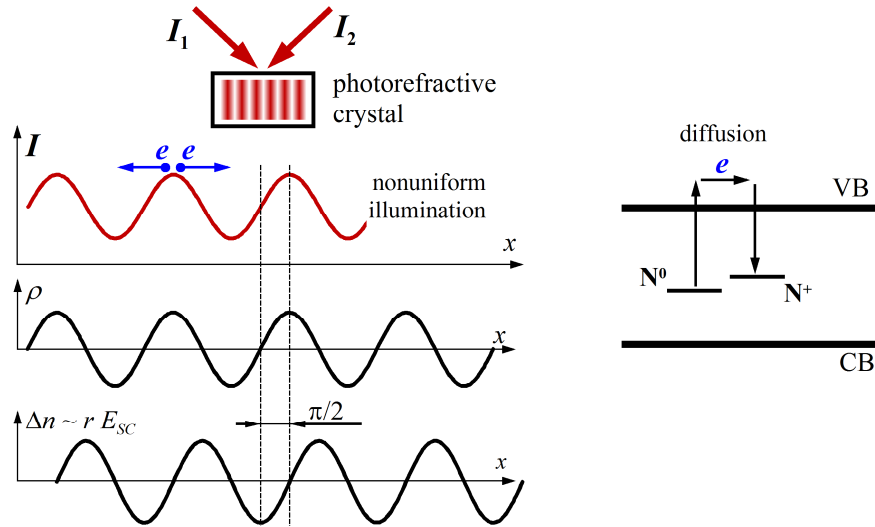


Figure 1. Schematic representation of the photorefractive recording.

Therefore the photorefractive material needs to be electro-optic with a large enough electro-optic coefficient. It should exhibit a low dark conductivity to be able to collect a space charge, but have a photoconductivity at the wavelength of operation. A large density of donors is necessary to supply the photoconductivity, while a large trap density is required for space charge formation. Generally, the same impurity or defect center in different charge states may serve as a donor and trap. Also, the free photo-excited carriers may be electrons or holes.

CdTe is the best material for adaptive interferometers because of the largest electro-optic coefficient among all semiconductors. It is sensitive at the eyesafe wavelength $\lambda = 1550$ nm, where modular and cost-effective telecommunications components are available. Some unique specially selected CdTe samples demonstrate the largest for semiconductors gain factor in photorefractive two-beam coupling at $\lambda = 1064$ nm and $\lambda = 1550$ nm¹³. The key feature for large donor and trap density is appropriate doping. Three elements are used mainly for enhancement of the photorefractive response of CdTe. These are vanadium¹⁴, germanium¹³ and tin¹⁵. If a comprehensive study of the space charge formation in vanadium¹⁶ and germanium¹⁷ doped crystals gave an understanding of the main processes involved long time ago, a similar study of CdTe:Sn was performed only recently⁷. In the present, work we extend results of this study and characterize CdTe:Sn as a material for TWM adaptive interferometry.

2. EXPERIMENTAL RESULTS AND DISCUSSION

The studied CdTe:Sn crystals were grown in Chernivtsy National University, Ukraine. The samples are rectangular in shape with typical dimensions $1 \times 0.5 \times 0.5$ cm³. The input optically polished faces are parallel to (110) plane, while the side faces are parallel to (001) plane. In the experiments requiring an external field, a voltage is applied to electrodes deposited on the side faces, forming an electric field E_0 along [001] axis. The crystals are deliberately doped. The initial tin concentration in the melt $N_{Sn} = 2.5 \times 10^{19}$ cm⁻³. A dark conductivity is estimated $\sigma_D < 1.7 \times 10^{-9}$ (Ohm \times cm)⁻¹.

2.1 Photorefractive properties at 1064 nm

Experimental set-up is shown schematically in Fig. 2. Continuous-wave laser radiation is divided by a beam splitter BS into two beams I_S^0 and I_P^0 with intensity ratio $\beta = I_P^0/I_S^0 \approx 100$. Both unexpanded beams enter the crystal through the face parallel to (110) plane, so that the grating vector \mathbf{K} is parallel to the [001] direction. The light polarization is perpendicular to the plane of incidence, i.e., it is parallel to [110] direction. The effective electro-optic coefficient is equal to the handbook value r_{41} in this geometry. The total light intensity is up to 500 mW/cm². To control the intensity, a variable attenuator is used. A phase electro-optic modulator EOM is used to control the grating recording and erasure.

It introduces in the pump wave packets of high-frequency sinusoidal oscillations $\varphi(t) = \Delta\varphi\sin(2\pi ft)$ with amplitude $\Delta\varphi = 2.4$ rad (the first zero of the zero order Bessel function $J_0(\Delta\varphi) \approx 0$). Such phase modulation stops the grating recording keeping the same averaged light intensity in the sample⁷. The gain factor $\Gamma = (1/d) \ln(I_S/I_S^0)$ is measured, where I_S^0 and I_S are the signal beam intensities behind the crystal with and without the fast phase modulation, respectively, and d is the interaction length.

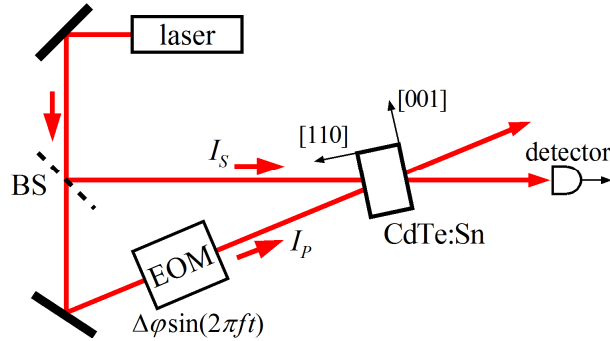


Figure 2. Experimental setup; BS – beam-splitter, EOM – electro-optic modulator.

The photorefractive recording is a light-induced process, which saturates with intensity. Therefore a certain intensity is necessary for grating formation with maximum index modulation. To estimate this intensity the gain factor is measured as a function of total light intensity at grating spacing $\Lambda = 1.1 \mu\text{m}$. Experimental data are shown in Fig. 3(a) by diamonds.

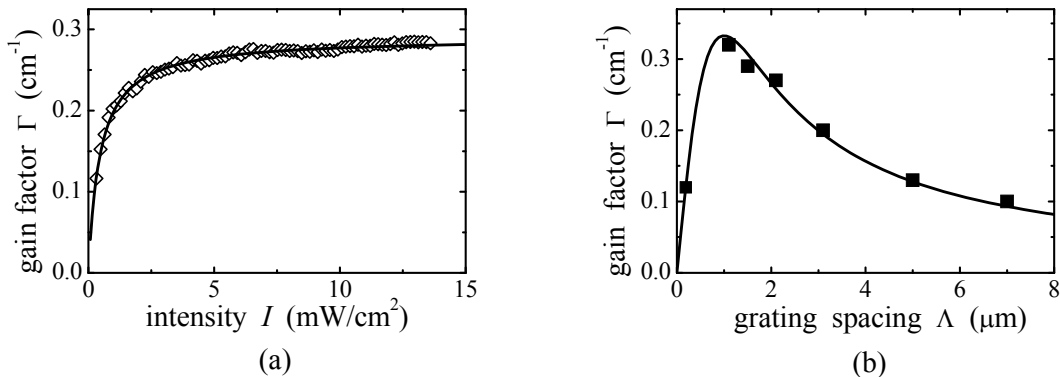


Figure 3. Gain factor versus (a) – recording light intensity, $\Lambda = 1.1 \mu\text{m}$; (b) – grating spacing.

The gain factor approaches saturation at quite small intensity $I = 3 \text{ mW/cm}^2$. For a simple one-level model of the photorefractive recording the intensity dependence of the gain factor has the form¹⁸

$$\Gamma = \Gamma_0 / (1 + \sigma_D / (\kappa I)), \tag{1}$$

where Γ_0 is the gain factor in saturation, σ_D is the dark conductivity, and κ is the specific photoconductivity. The line in Fig. 3a represents the best fit of Eq. (1) to the experimental data with $\Gamma_0 = 0.29 \text{ cm}^{-1}$ and $\sigma_D/\kappa = 0.46 \text{ mW/cm}^2$. The latter parameter has an important physical meaning. It defines the intensity, at which the photoconductivity becomes equal to the dark conductivity. The value, which is more than one order of magnitude better than that reported for CdTe:Ge¹³, demonstrates large photo-sensitivity of CdTe:Sn.

The maximum gain factor is reached in the diffusion mode of recording at a grating spacing equal to the Debye screening length¹⁰ ℓ_S

$$\Gamma = \frac{4\pi^2 n^3 r}{\lambda} \xi \frac{kT}{e} \frac{\Lambda}{\Lambda^2 + \ell_s^2}, \quad (2)$$

where n is unperturbed refractive index, r is electro-optic coefficient ($r = r_{41}$ in the present two-beam coupling geometry), k is the Boltzmann constant, T is the absolute temperature, e is the electron charge, ξ is the electron-hole competition factor, which takes into account a possible compensation of the main grating by secondary charge carriers, $\ell_s^2 = (4\pi^2 \epsilon \epsilon_0 kT)/(e^2 N_E)$, ϵ and ϵ_0 are the dielectric constants of material and vacuum, respectively, and N_E is the effective trap density. To estimate the Debye screening length and the effective trap density the gain factor is measured versus grating spacing. Experimental data are shown in Fig. 3b by squares. The line shows best fit of Eq. (2) to the experimental values with $\ell_s = 1 \mu\text{m}$ ($N_E = 6.2 \times 10^{14} \text{ cm}^{-3}$) and $\xi = 0.52$. Thus, analysis of the photorefractive measurements allows for estimation of the crystal characteristics and predicts that increase of the effective trap density is effective way for strengthening the photorefractive response in CdTe:Sn.

2.2 Magneto-optical study

A deeper understanding of the space charge formation and identification of the centers involved in the process may help to find ways for increasing of the effective trap density. Spectroscopic and magneto-optical studies are held for that purpose.

At least two tin related centers are expected in CdTe:Sn. These are the neutral Sn^0 (Sn^{2+} in the ionic notation) and the ionized Sn^+ (Sn^{3+}). The ionized Sn^+ is paramagnetic. Therefore it can be identified with magneto-optical techniques. One of the techniques is the magnetic circular dichroism (MCD). MCD measures the absorption difference $\Delta\alpha$ for the clockwise and counterclockwise circularly polarized light in the presence of a magnetic field B aligned along the light propagation. It resolves the absorption bands related to paramagnetic species at low temperature. The MCD spectrum measured at $T = 1.4 \text{ K}$ under magnetic field $B = 2.5 \text{ T}$ is shown in Fig. 4a. The negative band with a minimum at photon energy $E = 1.14 \text{ eV}$ is of particular interest because the levels in the middle of the gap are important for photorefraction.

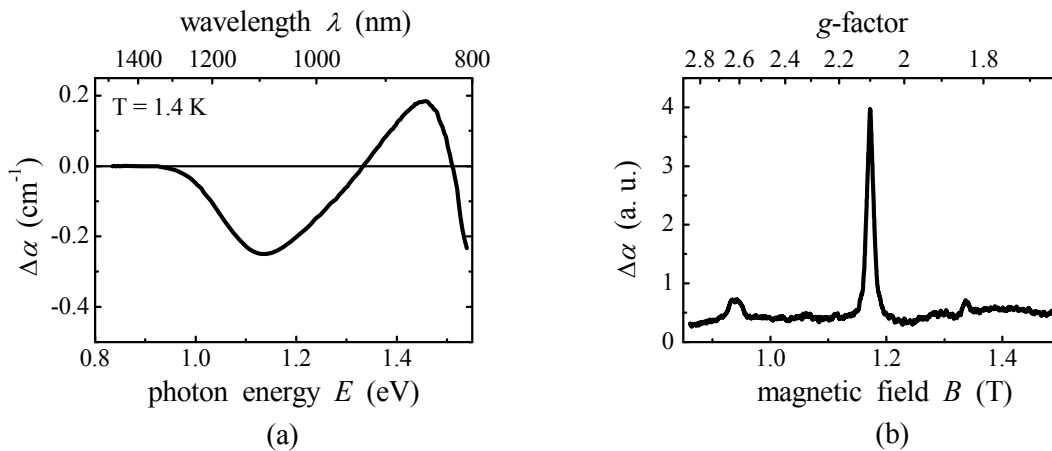


Figure 4. (a) – MCD spectrum measured at $T = 1.4 \text{ K}$ with $B = 2.5 \text{ T}$; (b) – ODMR measured with photon energy $E = 1 \text{ eV}$ in the presence of microwaves with $f = 34.45 \text{ GHz}$.

Optical Detection of Magnetic Resonance (ODMR) can assign the MCD band to a particular impurity center. ODMR measures MCD signal at a fixed wavelength as a function of magnetic field in the presence of microwaves. When Zeeman splitting matches the microwave photon energy, a resonant absorption of the microwaves occurs. A dip in the smooth curve $\Delta\alpha = f(B)$ is observed. The Landé g -factor can be evaluated from the resonance magnetic field. Then the absorption band can be attributed to particular paramagnetic center with known g -factor.

To identify the MCD band at $E = 1.14 \text{ eV}$ the ODMR is measured with photon energy 1 eV in the presence of microwaves with frequency $f = 34.45 \text{ GHz}$. The dependence shown in Fig. 4b exhibits sharp resonance at $B \approx 1.18 \text{ T}$,

which corresponds to $g = 2.1$. Paramagnetic tin Sn^+ in CdTe has been identified earlier by EPR¹⁹ with the isotropic Landé factor $g = 2.101$. Therefore the MCD band at $E = 1.14$ eV can undoubtedly be attributed to recharging of the ionized tin Sn^+ into its neutral state Sn^0 . The free holes are generated in this case under illumination.

The results of the magneto-optical experiments together with the data of photo-induced absorption studied in CdTe:Sn⁷ allows for estimation of the optical ionization energy $E = 1.09$ eV for tin in neutral state, Sn^0 . Additional photorefractive experiments show that the main charge carriers participating in the grating recording at $\lambda = 1064$ nm are holes. Strong overlapping of two absorption bands related to tin in different charge states results in strong electron-hole competition ($|\xi| < 1$) during the grating recording and explains moderate gain factor reported for the crystal. The larger gain factor can be reached with proper compensation of the influence of one of the species. An appropriate co-doping or modification of the crystal growth technique can be used for the suppressing destructive influence of secondary carriers.

2.3 Two-wave mixing adaptive interferometer with CdTe:Sn

Optical excitation energies for tin in different charge states fits perfectly to the radiation with $\lambda = 1064$ nm. Taking into account that the absorption bands related to the tin in semiconductor CdTe are broad at room temperature, we can expect effective photorefractive recording at $\lambda = 1550$ nm (photon energy $E = 0.8$ eV). To test this assumption we study TWM adaptive interferometer at this wavelength.

The experimental set-up is similar to that shown in Fig. 2, which is used for photorefractive experiments at $\lambda = 1064$ nm, with the following modifications. A continuous wave single frequency laser diode emitting at $\lambda = 1550$ nm serves as a light source. The intensity ratio of the recording beams $\beta \approx 10$. An external dc voltage is applied to the side faces of the crystal, forming an electric field along [001] axis. The EOM simulates ultrasonic surface displacements introducing in the signal wave fast phase modulation $\varphi(t) = \Delta\varphi \sin(2\pi ft)$ with low amplitude ($\Delta\varphi = 0.15$ rad $\ll \pi/2$ rad) and high frequency ($f = 50$ kHz $\gg 1/(2\pi\tau_{SC})$, τ_{SC} is response time of the grating). The phase modulation is transformed into intensity modulation of the signal beam behind the crystal. The amplitude of intensity modulation is measured at different experimental conditions.

An important feature of the adaptive interferometer is the ability to compensate for perturbations in environment. It is characterized by frequency range of the compensation, which can be represented by the amplitude of intensity modulation versus modulation frequency. Such dependence measured at grating spacing $\Lambda = 55$ μm with dc field $E_0 = 6$ kV/cm and total light intensity $I = 30$ mW/cm² is shown in Fig. 5a. The amplitude of intensity modulation ΔI_S is normalized by the intensity of the signal I_S^{mean} measured with no phase modulation.

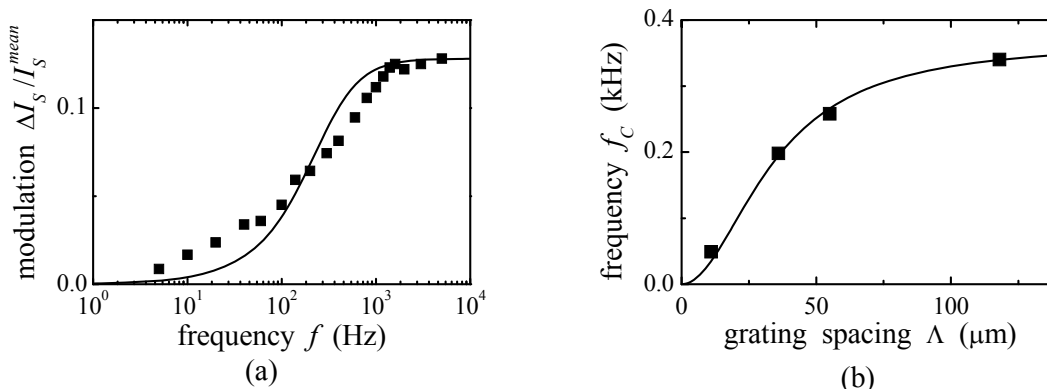


Figure 5. (a) – intensity modulation at the output of TWM interferometer versus frequency of the input phase modulation; (b) – cutoff frequency versus grating spacing.

The dependence in Fig. 5a has the typical shape of high-pass filter with cutoff frequency $f_c \approx 200$ Hz, which is defined at half level of the maximum intensity modulation at high frequency ΔI_S^{sat} . For a simple one-center model of the space charge formation it has the form

$$\Delta I_S = \Delta I_S^{sat} \frac{2\pi f \tau_{SC}}{\sqrt{1 + (2\pi f \tau_{SC})^2}}. \quad (3)$$

The line in Fig. 5a represents the best fit of Eq. (3) to the experimental data with $\tau_{SC} = 500 \mu\text{s}$ and a maximum modulation amplitude $\Delta I_S^{sat}/I_S^{mean} \approx 0.13$. The low frequency tail with increased response may be explained by a complex process of the space charge formation, which becomes more complicated at $\lambda = 1550 \text{ nm}$. The increased response at low frequency can perhaps be suppressed by temperature control of the crystal slightly above the room temperature, as it has been demonstrated for CdTe:Ge²⁰.

The photorefractive response time τ_{SC} changes strongly with the grating spacing¹⁰. For the diffusion length smaller than the drift length $L_D = (\mu\tau kT/e)^{1/2} \ll L_E = \mu\tau E_0$, the grating response time $\tau_{SC} = \tau_M(1 + 4\pi^2 K^2/\Lambda^2)$, where μ and τ are the mobility and lifetime of free charge carriers and τ_M is the dielectric response time of the crystal. Correspondingly, the cutoff frequency changes with the grating spacing as²⁰

$$f_C = \frac{1}{\sqrt{3}} \frac{1}{2\pi \tau_M (1 + 4\pi^2 L_E^2/\Lambda^2)}. \quad (4)$$

Therefore the study of cutoff frequency versus grating spacing may give information about the diffusion length and dielectric response time of the crystal. Such an experimental dependence is presented in Fig. 5b by squares. The line represents fitting calculation according Eq. (4) with $\tau_M = 250 \mu\text{s}$, $L_E = 5.4 \mu\text{m}$. The product $\mu\tau = 9 \times 10^{-8} \text{ cm}^2/\text{V}$ is estimated from the drift length.

The sensitivity of the adaptive interferometer to a small surface displacement is characterized usually by the relative detection limit. It is defined as the ratio of sensitivity of an adaptive interferometer to that of a classical lossless interferometer operating with plane waves. Assuming the losses of adaptive interferometer are minimized by means of antireflection coatings, etc., the relative detection limit can be estimated experimentally⁸

$$\delta_{rel} = \frac{\exp(\alpha d/2)}{|\sin(\gamma'' d)|}, \quad (5)$$

where α is the absorption constant and γ'' is the coupling constant of the local grating in dc-biased CdTe:Sn. The relative sensitivity $\delta_{rel} = 2.3$ is estimated using the measured absorption $\alpha d \approx 0.4$ and coupling strength $\gamma'' d \approx 0.56$ achieved with $E_0 = 8 \text{ kV/cm}$. This relative detection limit is equal to the value reported for CdTe:Ge²⁰, which is the best to our knowledge ever reported for adaptive interferometers at $\lambda = 1550 \text{ nm}$. Thus CdTe:Sn demonstrates excellent performance in TWM adaptive interferometer.

3. CONCLUSIONS

A comprehensive study of CdTe:Sn crystal using dynamic holography, optical spectroscopy and light-induced spectroscopy, MCD and ODMR shows that the space-charge formation is occurring within one-center model of the photorefractive recording. Analysis of the experimental results allows for estimation of optical activation energies of tin impurity center in two charge states: $E = 1.09 \text{ eV}$ for Sn^0 and $E = 1.14 \text{ eV}$ for Sn^+ . Different characteristics expressing charge transport in CdTe:Sn ($\ell_S, N_E, L_E, \mu\tau, \kappa/\sigma_D$) are evaluated. While CdTe:Sn demonstrates moderate photorefractive coupling constants with no external field, these coupling constants are achieved at low intensity of couple of mW/cm^2 . Such large photosensitivity and fast response makes CdTe:Sn promising material for applications. It is shown that adaptive interferometer with CdTe:Sn demonstrates good frequency response and the best sensitivity at $\lambda = 1550 \text{ nm}$. In addition, our studies show that a larger photorefractive response is expected in CdTe:Sn with reduced impact of the tin impurity center in one of its charge states. A targeted modification of the crystal synthesis process should be explored for such improvement of photorefractive CdTe:Sn.

4. ACKNOWLEDGEMENTS

Partial financial support of the European Office of Aerospace Research & Development (grant 118006) through the Science and Technology Center in Ukraine (Project P585a) is gratefully acknowledged. The authors thank Z. I. Zakharuk for the CdTe:Sn crystal.

REFERENCES

- [1] Davidson, F. M. and Boutsikaris, L., "Homodyne detection using photorefractive materials as beamsplitters," *Opt. Eng.* 29(4), 369-377 (1990).
- [2] Rossomakhin I. M. and Stepanov, S. I., "Linear adaptive interferometers via diffusion recording in cubic photorefractive crystals," *Opt. Commun.* 86(2), 199-204 (1991).
- [3] Ing, R. K. and Monchalin, J. P., "Broadband optical detection of ultrasound by two-wave mixing in a photorefractive crystal," *Appl. Phys. Lett.* 59(25), 3233-3235 (1991).
- [4] Bortolozzo, U., Residori, S. and Huignard, J. P., "Adaptive holography in liquid crystal light-valves," *Materials* 5(9), 1546-1559 (2012).
- [5] Jayet, B., Huignard, J. P. and Ramaz, F., "Refractive index and gain grating in Nd:YVO₄: application to speckle vibrometry and photoacoustic detection," *Opt. Lett.* 42(4), 695-698 (2017).
- [6] Bortolozzo, U., Dolfi, D., Huignard, J. P., Molin, S., Peigné, A. and Residori, S., "Self-adaptive vibrometry with CMOS-LCOS digital holography," *Opt. Lett.* 40(7), 1302-1305 (2015).
- [7] Shcherbin, K., Odoulov, S., Ramaz, F., Evans, D. R. and Briat, B., "Photosensitive center in CdTe:Sn: photorefractive, spectroscopic, and magneto-optical studies," *J. Opt. Soc. Am. B* 35(8), 2036-2045 (2018).
- [8] de Montmorillon, L. A., Delaye, Ph., Launay, J. C. and Roosen, G., "Novel theoretical aspects on photorefractive ultrasonic detection and implementation of a sensor with an optimum sensitivity," *J. Appl. Phys.* 82(12), 5913-5922 (1997).
- [9] Sugg, B., Shcherbin, K. V. and Frejlich J., "Determination of the time constant of fast photorefractive materials using the phase modulation technique," *Appl. Phys. Lett.* 66(24), 3257-3259 (1995).
- [10] Petrov, M. P., Stepanov, S. I. and Khomenko, A. V., [Photorefractive Crystals in Coherent Optical Systems], Springer-Verlag, Berlin (1991).
- [11] Solymar, L., Webb, D. J. and Grunnet-Jepsen, A., [The Physics and Applications of Photorefractive Materials], Clarendon Press, Oxford (1996).
- [12] Stepanov, S. I., "Applications of photorefractive crystals," *Rep. Prog. Phys.* 57(1), 39-116 (1994).
- [13] Shcherbin, K., "High photorefractive gain at counterpropagating geometry in CdTe:Ge at 1.064 μm and 1.55 μm ," *Appl. Opt.* 48(2), 371-374 (2009).
- [14] Bylsma, R. B., Bridenbaugh, P. M., Olson, D. H. and Glass A. M., "Photorefractive properties of doped cadmium telluride," *Appl. Phys. Lett.* 51(12), 889-891 (1987).
- [15] Shcherbin, K., Volkov, V., Rudenko, V., Odoulov, S., Borshch, A., Zakharuk, Z. and Rarenko, I., "Photorefractive properties of CdTe:Sn," *phys. stat. sol. (a)* 183(2), 337-343 (2001).
- [16] de Montmorillon, L. A., Delaye, Ph., Roosen, G., Bou Rjeily, H., Ramaz, F., Briat, B., Gies, J. G., Zielinger, J. P., Tapiero, M., von Bardeleben, H. J., Arnoux, T. and Launay, J. C., "Correlation between microscopic properties and the photorefractive response for vanadium-doped CdTe," *J. Opt. Soc. Am. B* 13(10), 2341-2351 (1996).
- [17] Briat, B., Shcherbin, K., Farid, B. and Ramaz, F., "Optical and magneto-optical study of photorefractive germanium-doped cadmium telluride," *Opt. Commun.* 156(4-6), 337-340 (1998).
- [18] Kukhtarev, N. V., Markov, V. B., Odoulov, S. G., Soskin, M. S. and Vinetskii, V. L., "Holographic storage in electrooptic crystals. II. Beam coupling – light amplification," *Ferroelectrics* 22(1), 961-964 (1978).
- [19] Jantsch, W. and Hendorfer, G., "Characterization of deep levels in CdTe by photo-EPR and related techniques," *J. Cryst. Growth* 101(1-4), 404-413 (1990).
- [20] Shcherbin, K., Danylyuk, V. and Klein, M. B., "Characteristics of two-wave mixing adaptive interferometer with CdTe:Ge at 1.06 and 1.55 μm and improved temporal adaptability with temperature control," *Appl. Opt.* 52(12) 2729-2734 (2013).